Design and Application of a New Cell for *in Situ* Infrared Reflection–Absorption Spectroscopy Investigations of Metal–Atmosphere Interfaces

CH. KLEBER,* J. KATTNER, J. FRANK, H. HOFFMANN, M. KRAFT, and M. SCHREINER

Institute for Chemical Technologies and Analytics, Analytical Chemistry Division, Vienna University of Technology, Getreidemarkt 9/151, A-1060 Vienna, Austria (Ch.K., J.F., M.K., M.S.); Institute of Sciences and Technologies in Art, Academy of Fine Arts, Schillerplatz 3, A-1010 Vienna, Austria (Ch.K., M.S.); and Institute of Applied Synthetic Chemistry, Physical Inorganic Chemistry Division, Vienna University of Technology, Getreidemarkt 9/153, A-1060 Vienna, Austria (J.K., H.H.)

A new experimental setup for studying reactions occurring in the metal–atmosphere interface by applying *in situ* infrared reflection–absorption spectroscopy (IRRAS) is presented. It consists of a gas-mixing unit, where the moist air is generated with or without corrosive gases, the reaction cell for the *in situ* investigations, and an optical system coupled with a Fourier transform infrared (FT-IR) spectrometer. For testing the unit, a specimen of pure copper was used, where the growth of Cu_2O on the polished surface could be observed during time-resolved measurements in synthetic air containing 80% RH (relative humidity). For comparison of the experimental results obtained, a computer simulation program was developed in order to calculate the peak position, the peak height, the peak width, and the thickness of the surface layer formed during the atmospheric corrosion. The simulation software is based on the four-phase model of covered surfaces.

Index Headings: **Corrosion; *In situ* measurements; Infrared reflection–absorption spectroscopy; IRRAS; Weathering; Simulation; Calculations.**

INTRODUCTION

In situ investigations using infrared (IR) light are widely used and reported in the literature.[1–3] While these investigations mainly deal with investigations at liquid–metal interfaces, the study presented here explores *in situ* investigations of reactions caused by atmospheric corrosion occurring at metal–atmosphere interfaces. Investigating these reactions is of significant importance for the understanding of the mechanism of corrosion as well as for the determination of the occurring corrosion reaction rates. The *in situ* cells for the investigation of these reactions previously published[4,5] are different from the one presented here. In contrast to the cell presented here, the cells already described in the literature[4,5] consist of two zinc selenide (ZnSe) windows and a more simplified air supply.[4] Beyond this, the cell presented in Ref. 5 is linked with a quartz crystal microbalance (QCM), by which the system is linked with a vacuum exhaust, which results in a more complicated measuring system. Both types of previously presented cells[4,5] only have one air supply, while in the cell presented here, the moist air is introduced by two stainless steel tubes, arranged at right angles, providing turbulence near the sample surface. Thus, the corrosion rates occurring depend strongly on the flow conditions of the surrounding atmosphere.[6] Further, the cells previously presented[4,5] are not modifiable concerning the angle of incidence of the IR beam. The cell presented in this paper allows variation of the angle of incidence by operating the twist- and tilt-mounted mirrors as well as the cell itself, so that it is easily possible to investigate other materials such as glass or synthetics during weathering.

In general, a clean and freshly polished metal surface is covered immediately with water when exposed to humidified air. Consequently, the formation of metal oxides on the surface is often initiated, which can be observed by *in situ* infrared reflection–absorption spectroscopy (IRRAS). A structural characterization of the oxide films formed, as well as chemical identification, can be achieved by FT-IR transmission spectroscopy as well,[7] although this technique depends on the properties of the sample substrate. Second reflection interference can occur for a small substrate thickness and can impede the measurements of thin films. This problem can be circumvented by performing Brewster angle measurements[8] for a substrate with a constant refractive index in the region of interest. The important advantage of IRRAS is that the absorbance of a thin film can be measured on any substrate as long as the roughness is low. Optical effects such as peak shift and loss of peak symmetry possibly distort the measured spectrum from the calculated values and should always be taken into consideration. These effects occur especially during measurements in the reflection mode of thick films with a high imaginary refractive index and for broad absorption bands.[4,9] However, such

Received 25 June 2002; accepted 23 August 2002.
* Author to whom correspondence should be sent. E-mail address: chkleber@iac.tuwien.ac.at.

0003-7028/03/5701-0088$2.00/0

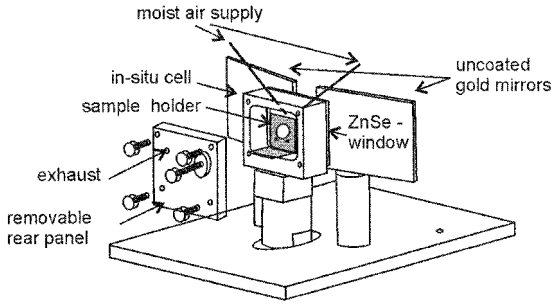

FIG. 1. Scheme of the constructed *in situ* cell consisting of acrylic glass with a removable rear panel, a ZnSe window, gas in- and outlets, and the external optical part with two uncoated gold mirrors.

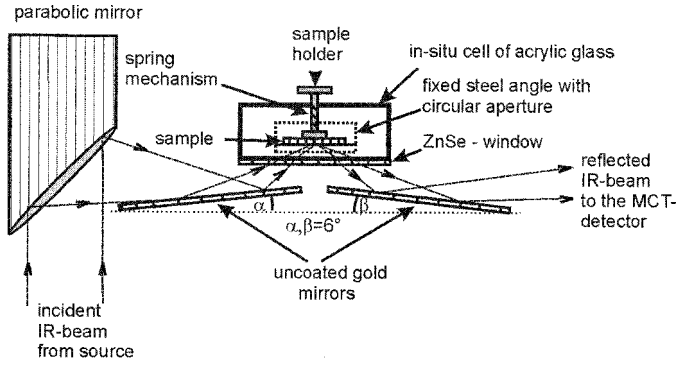

FIG. 2. Simulation of the pathway of the infrared beam in the cell.

phenomena can easily be determined since the peak position of an absorption band in a reflection experiment is shifted in comparison to the spectrum obtained in transmission mode or when the absorption band measured in the reflection mode shows some asymmetry.

The experimental setup presented enables *in situ* time-resolved monitoring of the reactions occurring at the early stages of atmospheric corrosion and is thus a valuable tool for a better understanding of the weathering reactions taking place in the ambient atmosphere.

EXPERIMENTAL

Design of the *in Situ* Cell. Figure 1 shows the developed *in situ* cell. It consists of acrylic glass with gas in- and outlets, a sample holder, a zinc selenide (ZnSe, cutoff at 500 cm^{-1}) window, and a rear panel, which can be unscrewed and to which a small cock with a spring mechanism is attached. The construction of the sample holder ensures that the sample cannot shift out of its position during the experiments. Therefore, it consists of a fixed steel angle with a circular aperture, in which the sample is placed from the back with the aid of the spring mechanism in the rear panel. The moist air is supplied through two stainless steel tubes, which are arranged at right angles in order to create turbulence near the sample surface by the incoming moist air. The uncoated gold mirrors can rotate and tilt and are mounted on the base plate. The system is constructed for an angle of incidence of 78° off the surface normal. The construction of the system was simulated by calculations using the software Optica® (Version 1.0; Optica Software, Urbana, IL) in combination with Mathematica® (Version 4.0; Wolfram Research Inc., Champaign, IL). The simulation took place for wavelengths between 2.5 and 20 μm. The geometry of the simulated components (apex angle of the incoming beam, distances between the components, and the diameter of the exit aperture) corresponds with the real conditions in the FT-IR spectrometer. The incoming beam was simulated by using a polychromatic light beam with a circular cross section and a suitable off-axis parabolic mirror. The uncoated gold mirrors used in the experimental setup were treated as ideal mirrors in the simulation, which is a tolerable approximation. Furthermore, an ideal mirror was taken as a sample for the simulations. For the calculation of the lateral offset of the IR beam in the ZnSe window, a ZnSe window without anti-reflection coatings was employed for the simulations. For this purpose, the refraction index model of the software Optica® was applied.

Figure 2 shows the simulated optical pathway, in which the optical properties of the materials used were taken into consideration as well. The ''one ZnSe window'' cell developed by us represents a new type of *in situ* cell due to the fact that all the cells described in the literature consist of two ZnSe windows.[4,5] The advantage of the ''one ZnSe window'' cell is, on one hand, a more simple design and, on the other hand, a reduction of the inner volume, which provides a better and faster distribution of the weathering gases in the cell. This is vital due to the fact that the predominant flow conditions in the cell and on the sample surface are of great importance for the occurring corrosion rates. Another important factor for applying a ''one ZnSe window'' cell is the higher intensity on the detector due to the reduced reflection and absorption losses by the ZnSe windows, whereby a better shot-to-noise ratio can be obtained.

Another advantage of the cell presented is that the air supply, which is split into two separate streams, provides turbulence near the sample surface as described above. The cells described in the literature[4,5] usually have only one gas inlet, which has to be mounted—with respect to the bigger dimensions of the two ZnSe window cells—at larger distances from the sample surface. This may negatively effect the flow conditions and flow velocity of the gas stream used. Additionally, the IR beam hits the ZnSe window at a perpendicular angle, whereas in the cell presented, a grinding wave angle is obtained. This is not a disadvantage as the reflectivity of ZnSe for *p*-polarized light is similar for an angle of incidence of 0° and of 78° off normal.[10]

Instrumentation for *in Situ* Infrared Reflection–Absorption Spectroscopy Measurements. The experimental setup used for the investigations consists of a Perkin Elmer Spectrum 2000 spectrometer with an optical module fitted with the source for the infrared light, a B-stop aperture (defining the area of the beam passing through the interferometer; it also controls the convergence of the beam at the sample position and is built as a variable iris aperture), the J-stop (improving the parallelism of the collimated beam and thus affecting the resolution of the instrument), and an interferometer. The IR beam coming from the interferometer has a diameter of 4 cm and the size in the focal point is 0.6 cm. The *in situ* cell, with an external optical part, is fitted in the sample chamber of the FT-IR instrument. A KRS-5 polarizer is placed before

the beam enters the detector area, in which a wide-band mercury cadmium telluride (MCT) detector (cutoff, 500 cm^{-1}) is placed.

The apparatus for generating moist air with or without a specific amount of corrosive gases such as SO_2 or NO_2 is described elsewhere.[11] By separating a dry air stream (Air Liquide Austria; synthetic Air 5.0, hydrocarbon-free) into two separate streams, where one is conducted to a bottle with purified water (Millipore, Milli-Q®), the desired level of humidity is achieved afterwards by mixing the two gas flows. The relative humidity of the exiting gas can be measured in the exhaust stream by a hygrometer. For corrosion studies under acidifying gases such as SO_2 or NO_2, the desired amount of SO_2 and NO_2 is added to the humidified air stream. The humidity can be regulated between 1 and 90% relative humidity, and the concentration of SO_2 and NO_2 can be varied from 125 to 500 ppb (parts per billion, 10^{-9} volume parts) with a maximum flow rate of 0.6 L/min. The maximum flow rate leads to a mean residence time of the moist air in the cell of approximately 2.4 s, as the inner volume of the *in situ* cell is approximately 26 cm^3.

Sample Preparation and *in Situ* Infrared Reflection–Absorption Spectroscopy Measurements. For the *in situ* experiments in the new setup, pure copper (Johnson Matthey, Paris/France, max. 25 ppm trace metal impurities) was used with a maximum diameter of the samples of 2 cm. The specimens were mechanically abraded with different SiC papers with roughness rates up to 2400 mesh, cleaned ultrasonically in ethanol absolute p.a., abraded afterwards with SiC of 4000 mesh, and cleaned again in ethanol. After this procedure, the samples were polished twice with 1 μm polycrystalline diamond paste (Struers, DP paste P), cleaned in ethanol, and, finally, polished twice with 0.25 μm polycrystalline diamond paste (Struers, DP paste P). After a final ultrasonic cleaning in ethanol the samples were flushed with dry nitrogen and transferred immediately to the *in situ* cell. The cell and the components of the FT-IR spectrometer (optical module, sample area, detector unit) were flushed with 40 L/h dry synthetic air (Air Liquide Austria; synthetic Air 5.0, hydrocarbon-free) over a period of 30 min in order to remove all CO_2. The reference spectrum was recorded after this period, also in dry air. Afterwards, air with 80% relative humidity entered the cell with a flow rate of 0.6 L/min. The absorption spectra were recorded using *p*-polarized light and the following hardware settings: a B-stop of 21.2 mm and a J-stop of 6.34 mm. The scan resolution was 4 cm^{-1} by averaging 1000 scans. The use of these parameters leads to a measuring time of approximately 12 min. The spectra were recorded in absorbance format ($-\log_{10}R/R_0$), where R is the reflected intensity for a thin film of oxide and water on the metal surface and R_0 is the reflected intensity for the unexposed metal surface.

Spectral Simulations. The main reason for applying computer-based simulation programs is to determine the peak position by using ideal data from the literature as stated below.

The spectra simulations were carried out using a program based on a 2 × 2 transfer matrix formalism. The sample is modeled as a stack of parallel layers with perfectly smooth phase boundaries, as shown in Fig. 3. All

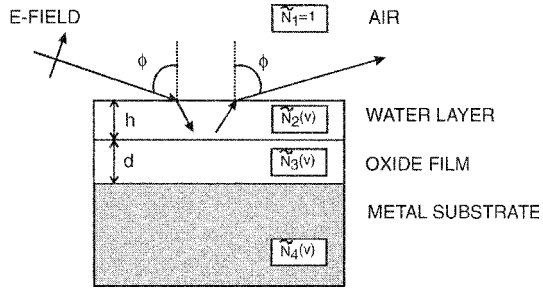

FIG. 3. Four-layer model with complex, frequency dependent, optical indices, on which the calculations of band sizes are based.

but the first and the last layer are optically characterized by their layer thickness and their complex refractive indices. The distinct layers confining the stack on both sides are assumed to be semi-infinite, i.e., the incidence medium and the substrate extend infinitely. The water layer in this model is 2.5 nm and the optical data for bulk water were taken from Ref. 12.

The transfer matrix formalism calculates the electrical field amplitudes at the phase boundaries between the layers. The relationship between the reflected and the incident amplitude yields the reflection coefficient r of the layer stack, which may be converted to the power reflectance R by the following equation:

$$R = |r|^2$$

All simulations were carried out for *p*-polarized light, where the electric field vector oscillates in the incidence plane of the radiation. The refractive index data were assumed to be isotropic (no birefringence); dispersion over the observed wavelength intervals was also taken into account by the use of discrete input data. Data for CuO and Cu_2O were taken from Ref. 13. Due to the absence of Cu complex refractive indices for wavenumbers below 1000 cm^{-1}, the data were extrapolated down to 400 cm^{-1} with data taken from Ref. 10. Further optical data for Cu[14] and Cu_2O[15] are given in the literature.

All calculated values are only exactly valid for (1) perfectly smooth surfaces and interfaces, and (2) for layers that exhibit the optical properties of the bulk materials. Due to scratches from sample preparation and surface recrystallization, condition (1) is not fulfilled. As long as the dimensions of the surface irregularities are well below the wavelength of the probing radiation, it encounters a smooth optical interference of the phases, which can be treated using effective medium approximations (EMA).[15] Due to the semi-quantitative nature of this investigation, this was not attempted here. Furthermore, the optical properties of ultra-thin films often deviate from the bulk properties. This can be due to stress, tension in the layers, the increased surface-to-volume ratio, and other factors. Consequently, differences in band positions and band intensities between simulated and experimental data must be expected. The available literature is ambiguous about the exact band positions themselves, so they can be expected to depend on the shape of the film.

In analogy to the literature,[16] a four-layer model was used for the simulations of oxide growth on copper: the bulk, infinitely extended copper substrate was covered by a growing Cu_2O layer and an additional layer of water

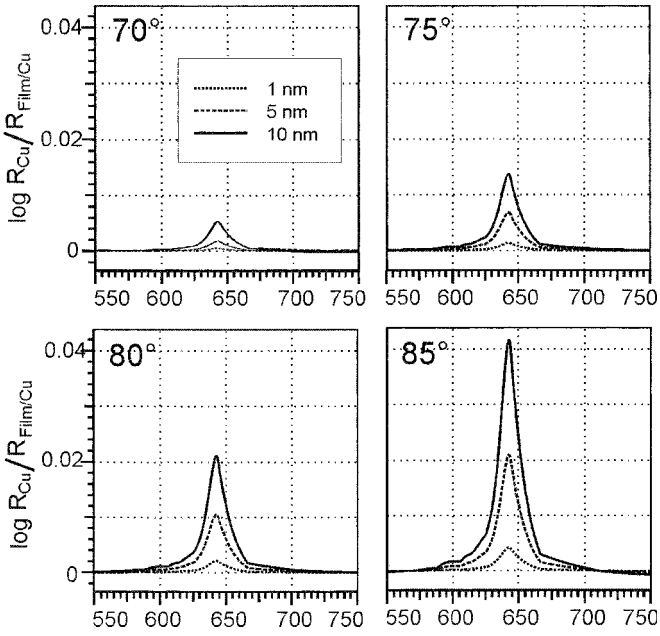

FIG. 4. Simulated spectra of Cu_2O on Cu in dependence on the angle of incidence and the layer thickness.

of constant thickness. The infinitely extended incidence medium is air.

Absorbance values were calculated by the ratio of the reflectivities of a blank copper substrate and the reflectivities of the sample consisting of the film and the additional layer of water.

Figure 4 shows simulated spectra for an adlayer of Cu_2O for different angles of incidence and different layer thicknesses.

Complementary *in Situ* Tapping Mode–Atomic Force Microscopy (TM-AFM) Measurements. The topography of the freshly polished sample surface as well as the two- and three-dimensional expansions of the features grown on the surface during weathering were determined by *in situ* TM-AFM measurements, as the corrosion products formed can influence the peak shifts and/or loss of peak symmetry. By such studies an imaging of the surface reactions occurring is obtained. The experimental setup of the *in situ* TM-AFM measurements is described elsewhere.[12]

RESULTS AND DISCUSSION

Figure 5a shows a freshly polished copper surface imaged *in situ* by TM-AFM. The scan size is 1 × 1 μm^2

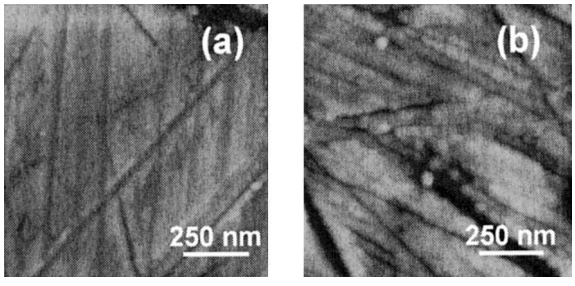

FIG. 5. TM-AFM images of (**a**) the freshly polished copper surface and (**b**) the weathered copper surface after 1120 min in 80% RH, in which the features grown during exposure are clearly visible (1 × 1 μm^2 scan size; z-range: 25 nm from black to white).

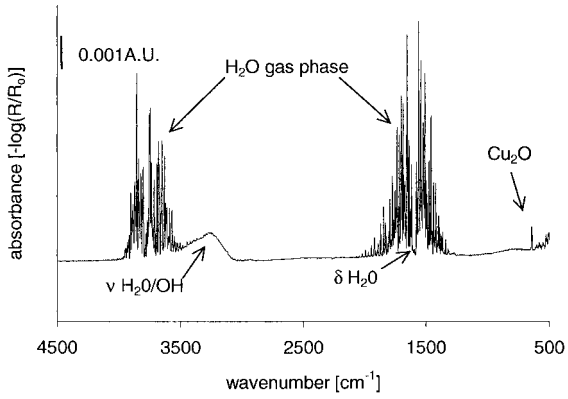

FIG. 6. IRRAS spectrum of copper exposed to 80% relative humidity showing the occurring absorbance bands. The background spectrum (R_0) was recorded in dry atmosphere.

and the black-to-white range is 25 nm. The scratches caused by the polishing process are clearly visible. It is also evident that the reference surface is not completely smooth, which may effect the position and shape of the bands obtained by the FT-IR *in situ* measurements. During weathering in 80% RH, round features appeared on the surface, which grew with time. After 1120 min of weathering, the features had diameters of approximately 50 nm, which implies a growth rate of the features of 0.04 nm/min (Fig. 5b).

Figure 6 depicts an unsmoothed IRRAS spectrum measured *in situ* on the copper surface, which was exposed to synthetic air with 80% RH for 512 minutes. The band at 640 cm^{-1}, which increases with time (see Fig. 7), corresponds to the formation of cuprous oxide,[17] hereafter referred to as Cu_2O. The Cu_2O band is shifted during weathering due to the surface disorder caused by the growth of the features (Fig. 5b). The band at 1600 cm^{-1} corresponds to the scissors vibration mode of water (δ), and the broad band at 3400 cm^{-1} corresponds to the symmetric and asymmetric stretching vibrations of water (ν), which is the OH group in water.[18] The latter band probably contains minor contributions of the hydroxylated surface. After turning off the humidity, the water bands

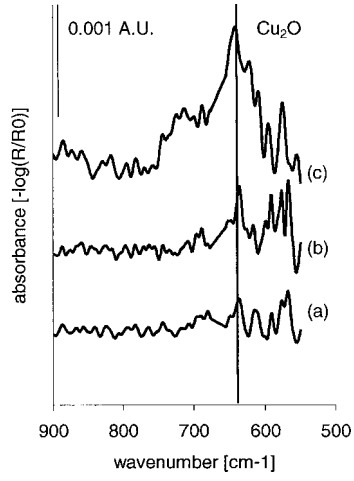

FIG. 7. Time-resolved *in situ* IRRAS spectra of copper exposed to 80% relative humidity. The growth of the Cu_2O band at 640 cm^{-1} (***a***) after 15 min, (***b***) after 45 min, and (***c***) after 1155 min of exposure are clearly visible.

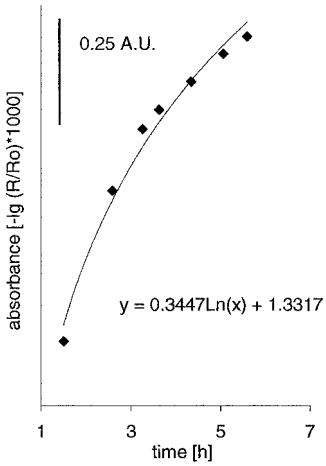

FIG. 8. Time dependence of the corrosion of copper in synthetic air with 80% RH using the areas of the Cu_2O bands at 645 cm^{-1}.

disappear in the spectrum, whereas the Cu_2O band could still be determined.

The fact that the Cu_2O band increases with time in the moist stream is clearly shown in Fig. 7. A comparison of the simulated and the measured spectra in Figs. 4 and 7, respectively, shows that the growth of the oxide layer yields an increased surface disorder resulting in a shifted peak of poor symmetry. Nevertheless, the simulation data are of great importance for the investigations, as the results received can give a hint to the position of a metal oxide peak.

Plotting the peak areas of the Cu_2O peaks, which increase with the duration of the weathering process, vs. time in a logarithmic scale (Fig. 8) leads to the conclusion that the early stages of corrosion of copper obey the logarithmic law described in the literature.[5]

CONCLUSION

A new cell for *in situ* IRRAS investigations of metal–atmosphere interfaces during atmospheric corrosion was built. The system consists of a unit for generating moist air with or without corrosive gases (such as SO_2 and NO_2) and a Perkin-Elmer Spectrum 2000 FT-IR spectrometer, in which the new cell with an external optical part is placed.

The cell presented here consists of polyacrylic glass as body material and is shut on the front with a ZnSe window. The air supply, to great advantage, is split into two separate streams, providing turbulence near the sample surface.

Copper samples were exposed to a synthetic air stream containing 80% relative humidity, whereby the time dependence of the formation of Cu_2O could be observed.

The cell presented here is ideal for *in situ* observations of the early stages of corrosion on metal surfaces. Therefore, it is a valuable tool for studying the surface reactions taking place during interactions of metals with the ambient atmosphere or under synthetic conditions.

1. D. D. Popenoe, S. M. Stole, and M. D. Porter, Appl. Spectrosc. **46,** 79 (1992).
2. H. Seki, K. Kunimatsu, and W. G. Golden, Appl. Spectrosc. **39,** 437 (1985).
3. B. O. Budevska and P. R. Griffiths, Anal. Chem. **65,** 2963 (1993).
4. D. Persson and C. Leygraf, J. Electrochem. Soc. **140,** 1256 (1993).
5. J. Itoh, T. Sasaki, T. Ohtsuka, and M. Osawa, J. Electroanal. Chem. **473,** 256 (1999).
6. T. E. Graedel, Corros. Sci. **38,** 2153 (1996).
7. P. A. Chollet and J. Messier, Chem. Phys. **73,** 235 (1982).
8. H. Ohshima and Y. Yamada, J. Appl. Phys. **32,** 1176 (1993).
9. A. Mielczarski, J. Phys. Chem. **97,** 2649 (1993).
10. D. Palik, *Handbook of Optical Constants of Solids* (Academic Press, New York, 1985), pp. 280–286.
11. Ch. Kleber, M. Rosner, H. Hutter, and M. Schreiner, J. Anal. Bioanal. Chem., paper accepted for publication (2002).
12. D. M. Wieliczka, S. Wenig, and M. R. Querry, Appl. Opt. **28,** 1714 (1989).
13. D. Palik, *Handbook of Optical Constants of Solids II* (Academic Press, New York, 1991), pp. 875–882.
14. M. A. Ordal, Appl. Opt. **22,** 1099 (1983).
15. M. O'Keeffe, J. Chem. Phys. **39,** 1789 (1963).
16. D. E. Aspnes, Thin Solid Films **89,** 249 (1982).
17. T. E. Graedel, Corros. Sci. **38,** 2153 (1996).
18. P. Eriksson, L. G. Johansson, and H. Strandberg, J. Electrochem. Soc. **53,** 140 (1993).
19. P. A. Thiel and T. E. Madey, Surf. Sci. Rep. **7,** 218 (1987).